

Petrography, geochemistry and Alteration Studies of Kanawa Uranium Occurrences, Wuyo-Gubrunde Horst, Northeastern Nigeria

Saleh Ibrahim Bute*

Department of Geology, Gombe State University, Nigeria

Abstract

The Kanawa uranium occurrence is situated along a northerly fault zone at Gubrunde horst, underlain by migmatites-gneiss, syntectonic S-type granites and minor volcanic rock. The sheared zone is highly altered. The alteration products are sericite, chlorite, and hematite. The uranium occurrences are epigenetic derived by remobilization from the host rock to the sheared zones, probably through metasomatic process where feldspars has been replaced by U-Fe-Mg in an oxidized conditions, the mineralizing fluids may be sourced from the numerous volcanic bodies around the area. The host rock showed enrichment of uranium >5, could serve as the potential source of the mineralization. The mineralized mylonite is a product of the granitic host. The Fe-Mg-Ca-P-Sr-Zr-V-Co-U may reflect mineralization fluid composition.

Keywords: Kanawa; Alteration; Uranium; Hematitic silica; Hematization

Introduction

Uranium is a mobile element, generally been classified as a lithophilic element which tends to accumulate at the later stage of magma crystallization. It may oxidize to hexavalent state as the complex uranyl (UO_2^{+2}), which permits extensive into two phases, the volatile and fluid phase. The mobility of uranium makes it difficult in search for economic deposits. Shallow accumulate of surface occurrence may portray false existence of buried deposits. The understanding of the fundamental geologic and geochemical processes that concentrate uranium and likely environment in which the ore occur is paramount important in the search for uranium in granitoids and associated rocks.

The uranium occurrences of Gubrunde horst have been worked for three decades but reasonable prospects have not yet been identified. There is a controversy on the rock hosting the uranium occurrences, for example Funtua et al. pointed out that the mineralized portion is altered/brecciated rhyolite while according to Suh and Dada, identified such mineralized portion as reddish hematitic silica, a product of deformed granites [1-3]. This paper discusses the alteration patterns, uranium mineralization and the host rock characterization using the new data on mineralogy and geochemistry of the host rocks and mineralized zone.

Geological Setting

The Kanawa uranium mineralization is located at Gubrunde Horst, Gubrunde Horst is a major structure in the Hawal massif which is believed to be a product of Lower Cretaceous block faulting between two series of NE-SW strike border faults which is bounded to the north and west by basalts of Biu and Cretaceous sediment respectively [1,3,4]. The horst is underlain by migmatites, granite gneiss, mafic and intermediate plutonic rocks syntectonic equigranular and porphyritic granites (Figure 1). The oldest rock units in the region are the migmatites and granite-gneiss with emplacement ages ranges between 680-620 Ma and 620-590 Ma, respectively [1,5]. Mesozoic-Tertiary magmatism have recorded giving rise to alkaline rhyolites and transitional alkaline basalts [4,6]. These volcanic rocks forms part of the Burashika bimodal volcanic Group [4].

The Cretaceous-Tertiary sedimentary rocks comprising sandstone, siltstone, limestones, shales and claystones. The Bima Formation

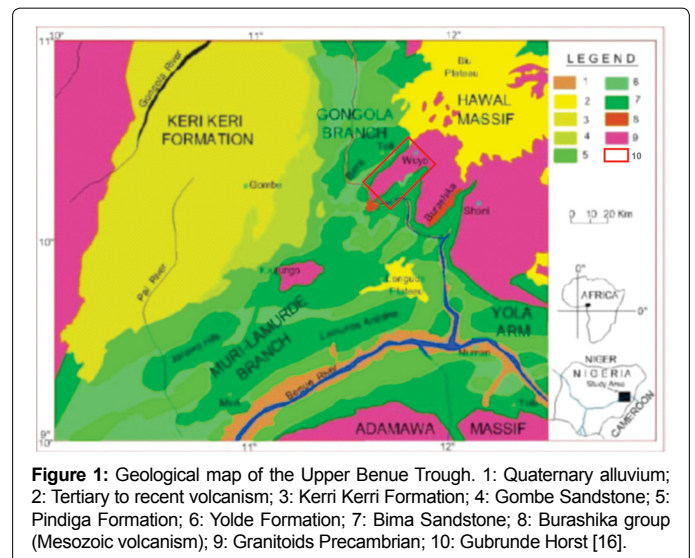


Figure 1: Geological map of the Upper Benue Trough. 1: Quaternary alluvium; 2: Tertiary to recent volcanism; 3: Kerri Kerri Formation; 4: Gombe Sandstone; 5: Pindiga Formation; 6: Yolde Formation; 7: Bima Sandstone; 8: Burashika group (Mesozoic volcanism); 9: Granitoids Precambrian; 10: Gubrunde Horst [16].

is the oldest lithologic unit occupying the base of the Cretaceous successions in the Northern Benue Trough; the sediments were mainly derived from juxtaposed basement rocks of older granites and gneisses and were deposited in a continental environment under widely varying conditions. The Yolde Formation lies conformably on the Bima Sandstone, represents the beginning of marine incursion into the Gongola Arm. The Turonian-Santonian Pindiga Formation conformably overlies the Yolde formation, which represents the full marine incursion in the Gongola arm [6,7]. The estuarine/deltaic Gombe Sandstone of Maastrichtian age overlies the Pindiga Formation

*Corresponding author: Saleh Ibrahim Bute, Department of Geology, Gombe State University, Nigeria; Tel: +234 813 072 8089; E-mail: salehbutee@yahoo.com

Received June 13, 2017; Accepted July 12, 2017; Published July 19, 2017

Citation: Bute SI (2017) Petrography, geochemistry and Alteration Studies of Kanawa Uranium Occurrences, Wuyo-Gubrunde Horst, Northeastern Nigeria. J Geol Geophys 6: 297. doi: [10.4172/2381-8719.1000297](https://doi.org/10.4172/2381-8719.1000297)

Copyright: © 2017 Bute SI. This is an open-access article distributed under the terms of the Creative Commons Attribution License, which permits unrestricted use, distribution, and reproduction in any medium, provided the original author and source are credited.

which represents the youngest Cretaceous sediments in the Gongola Arm [5]. The Paleocene Kerri-Kerri Formation unconformably overlies the Gombe Sandstone and represents the only record of Tertiary sedimentation in the Gongola Arm [8].

Methodology

Sixteen (16) rock samples were selected for thin section and were cut in a plane normal to the mylonitic foliation. The slides were studied at the petrology laboratory of the Department of Geology, University of Ibadan. A total of thirty (30) samples were selected and analyzed using the ICP-MS method for the analysis. The samples were analyzed for major, minor, and rare earth elements (REE) at ACME Laboratories, Vancouver, Canada. Aggressive fusion techniques employing lithium metaborate/tetraborate fusion was chosen for the analyses, precision for major elements is better than 2% and for trace elements is better than 5%.

Field and Petrographic Studies

The Wuyo area is underlain by migmatites, medium grained granite, porphyritic granite, basalts and Bima sandstone (Figure 2).

Migmatites

The migmatite gneiss portrays banding of felsic and mafic minerals alignment. The felsic minerals are mainly quartz and plagioclase while the mafic are hornblende and biotite which shows evidence of deformation, where the biotite is stretched enclosing the ellipsoidal plagioclase. Mineral associations are polycrystalline ribbon quartz, minor K-feldspars, augen plagioclase porphyroblast, development of myrmekites at grain boundaries is observed. Hornblende with biotite flakes makes up the mafic band containing small amount of euhedral inclusion of accessory minerals (Figure 3a).

Granites

The granites are medium grained to porphyritic granites. The striking characteristics of porphyritic granites are its porphyritic

texture consisting of microcline phenocryst. The medium grained granites are highly fractured blocks, blocks of medium grained granites are frequently found within the porphyritic granites implying the former were emplaced earlier than the latter (Figures 3b and 3c). Microscopically both the medium-grained and porphyritic granite display similar mineralogy (Table 1). They are composed of quartz, microcline, orthoclase, plagioclase with few mica shards, accessory minerals includes titanite, zircon, and apatite. Secondary alteration of micas to chlorite is observed. The feldspars are commonly deformed by transgranular fracturing.

Mylonites

The uranium occurrences is been hosted at the centre of nearly northerly trending sheared zone. This sheared zone is within the porphyritic granites which may have been derived from the precursor rocks and showed progressive increase in the intensity of deformation from the external limit (E-W) of the shear zones to the center. The mylonites contain stretched orthoclase and quartz porphyroblasts while the ellipsoid plagioclase are usually fragmented. The quartz grains portray stretched ribbon like features displaying undoluse extinction with sub-grains occurring as aggregate. The alteration observed moving E-S along N-S shear zone are kaolinization, silicification and hematization.

Basalts

There are several volcanic plugs in the study area; it contains olivines, labradorite laths, augite and iron oxides. The olivines are slightly serpentinised, with corona (Figure 3d).

Alteration studies

The alteration of feldspars may produce free ions such as Si^{4+} , Al^{3+} , K^+ , and Na^+ that can be easily remobilized together with the uranium. Evidence from the geochemical data, the inconsistency on the enrichment and depletion of alkalis, silica and iron oxide reflects

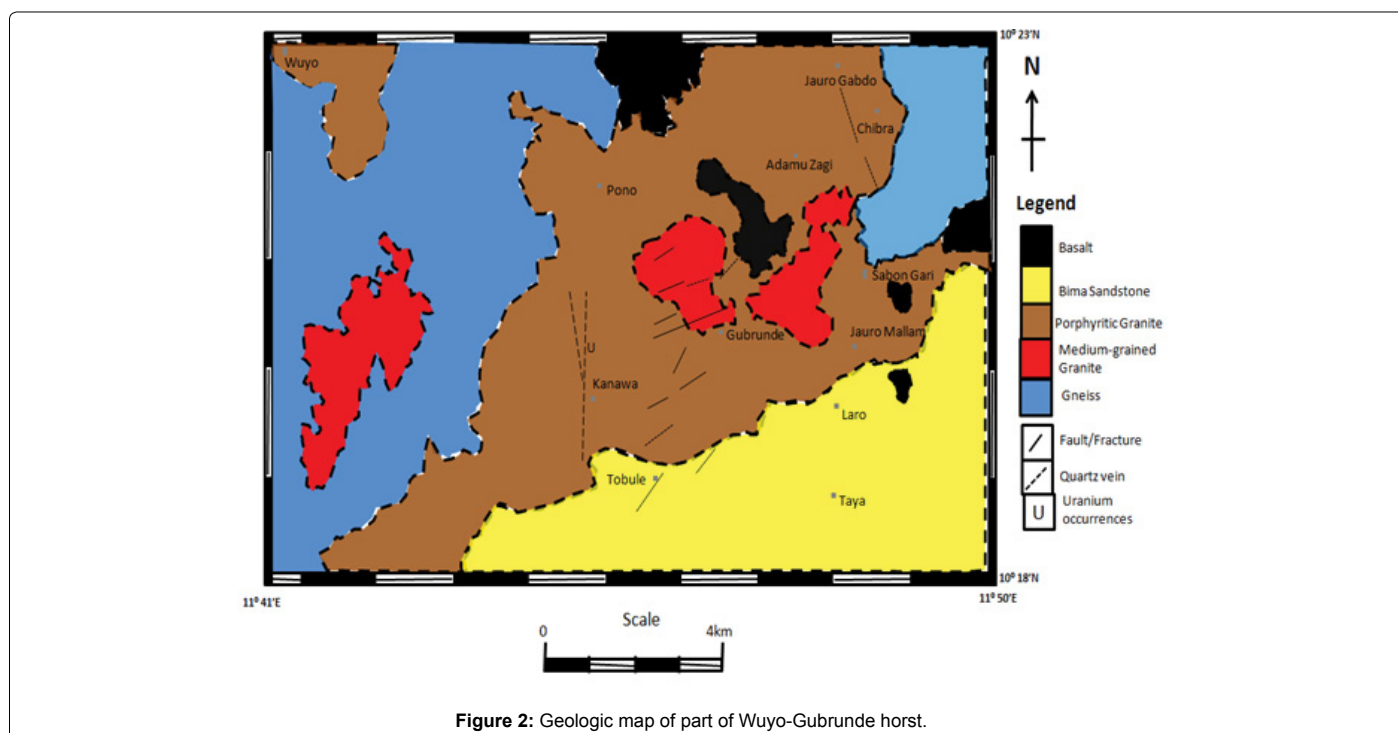


Figure 2: Geologic map of part of Wuyo-Gubrunde horst.

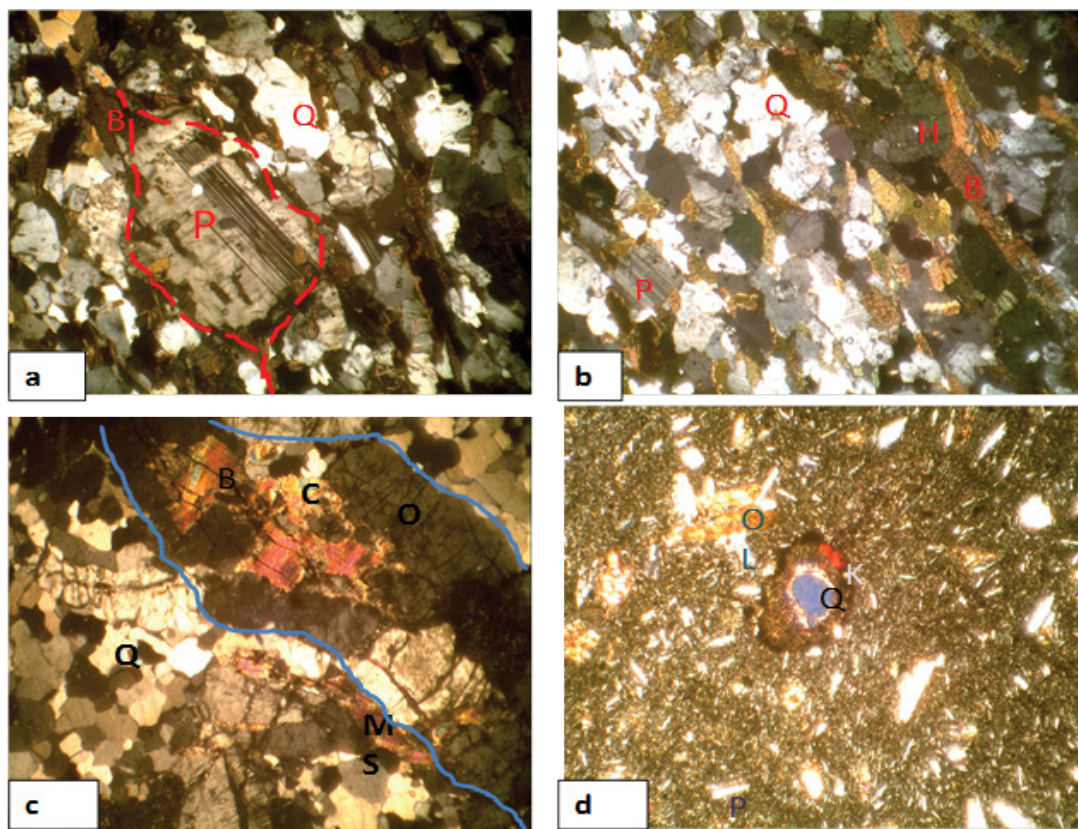


Figure 3: a) Augen plagioclase porphyroblast surrounded by stretched lenses of biotite crystals depicts plastic deformation; b) The banding character depicted by alignment of felsic and mafic minerals; c) Feldspar porphyroclasts depicting transgranular fracturing; d) Corona texture, large crystals of quartz was also observed. (Magnification 40X).

| Metal | Gneiss | Porphyritic Granite | Medium grained Granite | Basalt |
|-------------|--------|---------------------|------------------------|--------|
| Quartz | 30 | 30 | 35 | 5 |
| K-feldspar | 20 | 35 | 25 | - |
| Plagioclase | 15 | 13 | 25 | 30 |
| Biotite | 15 | 12 | 10 | - |
| Muscovite | - | 5 | - | - |
| Hornblende | 13 | - | - | - |
| Olivine | - | - | - | 20 |
| Augite | - | - | - | 10 |
| Opaque | 7 | 5 | 5 | 35 |

Table 1: Modal composition of the rock units in Wuyo-Gubrunde area.

remobilization of these elements. The mineralized mylonite is very poor in alkalis (<1), silica (<52), higher in $Fe_2O_3=18\%$, $Al_2O_3=15\%$, $P_2O_5=2.4\%$, uranium mineralization is associated with desilification and ferruginization. The Ishikawa (alteration index) AI, where elements gained during chlorite and sericite alteration ($MgO+K_2O$) over the elements loss and gain ($Na_2O+CaO+MgO+K_2O$) was used as reference in this study (Table 2) [9]. The chlorite-carbonate-pyrite index (CCPI), Mg-Fe chlorite altered is typically developed where hydrothermal temperatures and water/rock ratios are at their highest level. Mg-Fe chlorite development commonly replaces plagioclase, K-feldspars which have been observed at mineralized portion on the thin section the dominant minerals is reddish iron oxide mineral (hematite) leading to the loss of alkalis which is observed by its low alkalis value of Na_2O (0.09-2.7 wt%) and K_2O (0.03-4.18 wt%) as shown in Figure 4. The

migmatites, basalt and ferruginised mylonite falls within the truncated triangular field (carbonate-sericite \pm chlorite), where the AI varies from 3-52 and CCPI from 54-99.8. The porphyritic granites and silicified mylonites shows pervasive alteration typically exhibits $AI>85$ and $19<CCPI<60$. The aplites falls in the field of least altered (Figures 4a and 4b). The relationship between Na_2O and the AI in the granitoids, the depletion pattern of sodium with increase AI is outlined (Figure 5). The trend shows a shift from albite-plagioclase field to the chlorite-sericite corners evidence of pervasive alteration. Also K_2O enrichment typically exhibits increase in AI which is dependent on the ratio of sericite to chlorite in the altered product (Table 3).

Petrogenesis of Kanawa granitoids

Two types of granites is been recognized by Chappell and White, each related to a particular orogenic belt [10]. I-type granite which is compositionally expanded while the S-type granite are compositionally restricted. Both granites have distinctive petrochemical characteristics which reflect the differences in the sources of magma. The I-type granites are derived from basic igneous source by remelting of deep seated igneous material or the mantle, while the S-type granite are derived from melting of meta sedimentary source materials. The distinguishing mineralogical, petrochemical and field relationship of different sources as proposed by Chapell and White are compared with those of Wuyo-Gubrunde granitoids in Table 4 [10]. Such comparison showed that the granitoids shows that they are of S-type characteristics and support the model of its derivation by partial melting of meta sedimentary rocks in the crust.

| Rock | Granite gneiss | | Ferruginized mylonite | | Porphyritic granite | | | Silicified mylonite | | | Aplite | Basalt | | |
|--------------------------------|----------------|------------|-----------------------|------------|---------------------|-------|-------|---------------------|-------|-------|-------------|--------|-------|-------|
| | 1 n = 3 | 2 n = 3 | 3 n = 3 | 4 n = 3 | 5 | 6 | 7 | 8 | 9 | 10 | 11 n = 3 | 12 | 13 | 14 |
| SiO ₂ | 52.86 | 64.35 | 51.28 | 50.83 | 65.02 | 67.44 | 74.97 | 61.77 | 80.37 | 79.6 | 66.32 | 51.55 | 51.2 | 51.5 |
| TiO ₂ | 2.22 | 1.14 | 2.59 | 2.63 | 0.62 | 0.36 | 0.3 | 0.17 | 0.12 | 0.12 | 0.48 | 2.59 | 2.64 | 2.61 |
| Al ₂ O ₃ | 15.76 | 14 | 15.28 | 14.79 | 18.74 | 17.87 | 14.02 | 9.81 | 11.25 | 12.5 | 16.04 | 14.77 | 14.89 | 14.77 |
| Fe ₂ O ₃ | 10.16 | 6.88 | 16.8 | 18 | 4.33 | 3.33 | 1.94 | 1.08 | 1.5 | 1.71 | 3.42 | 11.62 | 11.64 | 11.6 |
| MnO | 0.15 | 0.09 | 0.51 | 0.38 | 0.06 | 0.04 | 0.01 | 0.02 | 0.01 | 0.01 | 0.08 | 0.13 | 0.13 | 0.12 |
| MgO | 3.76 | 1.61 | 0.08 | 0.07 | 0.89 | 0.12 | 0.22 | 0.09 | 0.22 | 0.24 | 1.05 | 5.72 | 5.83 | 5.83 |
| CaO | 6.48 | 3.07 | 3.12 | 3.22 | 0.35 | 0.33 | 0.1 | 17.81 | 0.07 | 0.14 | 1.59 | 7.79 | 7.83 | 7.8 |
| Na ₂ O | 2.73 | 2.6 | 0.01 | 0.02 | 0.11 | 0.13 | 0.12 | 0.12 | 0.09 | 0.06 | 3.34 | 3.16 | 3.18 | 3.18 |
| K ₂ O | 3.73 | 4.62 | 0.03 | 0.09 | 3.57 | 3.92 | 4.21 | 4.18 | 3.55 | 1.8 | 5.83 | 1.45 | 1.42 | 1.45 |
| P ₂ O ₅ | 0.69 | 0.49 | 2.34 | 2.31 | 0.21 | 0.15 | 0.09 | 0.07 | 0.04 | 0.05 | 0.24 | 0.4 | 0.43 | 0.42 |
| LOI | 1 | 0.7 | 7.7 | 7.4 | 5.9 | 6.1 | 3.9 | 4.8 | 2.7 | 3.7 | 1.4 | 0.5 | 0.5 | 0.6 |
| Total | 99.57 | 99.61 | 99.75 | 99.77 | 99.81 | 99.77 | 99.84 | 99.89 | 99.88 | 99.95 | 99.78 | 99.7 | 99.7 | 99.7 |
| Trace elements (ppm) | | | | | | | | | | | | | | |
| Ni | 21 | <20 | <20 | <20 | <20 | <20 | <20 | <20 | <20 | <20 | <20 | 121 | 122 | 121.5 |
| Co | 27.5 | 10.6 | 56.2 | 46.1 | 5.3 | 2.6 | 2.2 | 4.1 | 1.5 | 1.8 | 8.2 | 44.7 | 43.6 | 44.15 |
| Sc | 18 | 14 | 23 | 23 | 10 | 5 | 4 | 3 | 3 | 4 | 8 | 15 | 15 | 15 |
| V | 208 | 83 | 184 | 190 | 41 | 28 | 22 | 12 | 16 | 17 | 47 | 169 | 168 | 168.5 |
| Rb | 183.2 | 243.6 | 3.4 | 5.2 | 247.1 | 122.3 | 139.9 | 152.7 | 172.3 | 136.7 | 248.2 | 37.5 | 37.6 | 37.6 |
| Sr | 527.6 | 280.1 | 139.7 | 137.5 | 83.8 | 82.8 | 53.8 | 184.4 | 139.7 | 57 | 210.5 | 575.3 | 570.3 | 572.8 |
| Ba | 1065 | 894 | 306 | 196 | 442 | 986 | 865 | 495 | 703 | 131 | 504 | 368 | 372 | 372 |
| Zr | 577.4 | 756.6 | 501.2 | 482.7 | 355.6 | 367.2 | 196.3 | 85.8 | 63.7 | 81.2 | 316 | 192.5 | 192.4 | 192.4 |
| Nb | 36.6 | 33.1 | 45.5 | 44.6 | 20.2 | 19.8 | 9.5 | 6.6 | 6.4 | 10.5 | 19.3 | 37.7 | 38.9 | 38.3 |
| Ta | 2.1 | 3 | 2.7 | 2.6 | 1.5 | 1.4 | 0.5 | 0.4 | 0.6 | 1.1 | 1.5 | 2.4 | 2.4 | 2.4 |
| Sn | 4 | 12 | 2 | 2 | 12 | 5 | 4 | 2 | 4 | 5 | 13 | 3 | 3 | 3 |
| Be | <1 | 3 | 9 | 2 | 6 | 4 | 1 | 2 | 5 | 3 | 8 | 3 | <1 | 2 |
| W | 0.6 | 0.5 | 1.6 | 1.8 | 1.5 | 0.4 | 0.4 | 0.4 | 0.5 | 0.4 | 0.4 | 0.6 | 0.6 | 0.6 |
| Cs | 3.4 | 4.2 | 0.2 | 0.1 | 13.5 | 1.2 | 2.9 | 1.9 | 7 | 3.5 | 10.1 | 0.5 | 0.4 | 0.45 |
| Ga | 19.7 | 24.5 | 24.6 | 24 | 33.4 | 24.5 | 19.5 | 13.4 | 20.9 | 27.3 | 26.6 | 20.7 | 20 | 20.23 |
| Y | 43.5 | 42.4 | 70.6 | 70.2 | 37.3 | 20.4 | 9.7 | 27.9 | 7.9 | 24.8 | 21.9 | 22.4 | 22.15 | 22.5 |
| Hf | 14.3 | 19.6 | 11.6 | 10.9 | 10.7 | 10.1 | 5.5 | 2.7 | 2 | 2.6 | 9.8 | 4.7 | 4.7 | 4.7 |
| Th | 14.8 | 48.1 | 4.2 | 4.3 | 48.7 | 39.8 | 26.7 | 15.4 | 10.2 | 13.5 | 25.9 | 4.6 | 4.3 | 4.5 |
| U | 3.7 | 7.1 | 13.2 | 130.6 | 4.7 | 5.7 | 4.2 | 2.7 | 1.7 | 3.5 | 3.8 | 1.1 | 0.9 | 1 |
| Th/U | 4 | 6.78 | 0.31 | 0.31 | 10.26 | 7 | 6.35 | 5.7 | 6 | 3.86 | 6.83 | 4.18 | 4.78 | 4.45 |
| Rb/Sr | 0.34 | 0.87 | 0.03 | 0.04 | 2.95 | 1.48 | 2.6 | 0.83 | 1.23 | 2.4 | 1.17 | 0.07 | 0.07 | 0.07 |
| Al | 44.9 | 52.4 | 3.4 | 4.71 | 90.7 | 89.8 | 95.3 | 19.3 | 95.9 | 91.07 | 58.3 | 39.7 | 39.7 | 39.9 |
| CCPI | 68.3 | 54.1 | 99.8 | 99.4 | 58.7 | 46 | 33.3 | 21.4 | 32.1 | 51.18 | 32.8 | 79 | 79.1 | 79 |

Table 2: Major oxides compositions (wt %) and trace element (ppm) data of Wuyo-Gubrunde rocks [n=3-Number of samples analysed; Alteration Index (AI); Chlorite-carbonate-pyrite index (CCPI)].

Geochemistry of Kanawa uranium occurrence

Th/U ratio values of plutonic rocks ranges 4-6 reflects loss of uranium into the late-stage fluids, Th/U ratio is higher in porphyritic granites 7, the migmatites 5, aplite and basalt 5, 4 in silicified granites lowest in the mineralized zone 0.31. The oxidation of uranium is associated with loss in thorium which is clearly observed in this study, the mineralized portion is enriched with Fe₂O₃=18% and poor in Th=4.2 ppm.

The mineralized granitoids are S-type granites (Table 4) implying derived by remelting of pre-existing crustal material at a near depth of 20-30 km [11]. Remobilization of uranium from the surrounding host rock could be the likely source, U and Rb behave incompatibly in granitic melts; the kanawa uranium mineralization displays enrichment of U with loss in Rb (Figure 6) evidence of remobilization, magmatic sourced uranium on the hand shows positive correlation of Rb and U (Table 5) [12]. The variations in REE total values of the rocks (123-

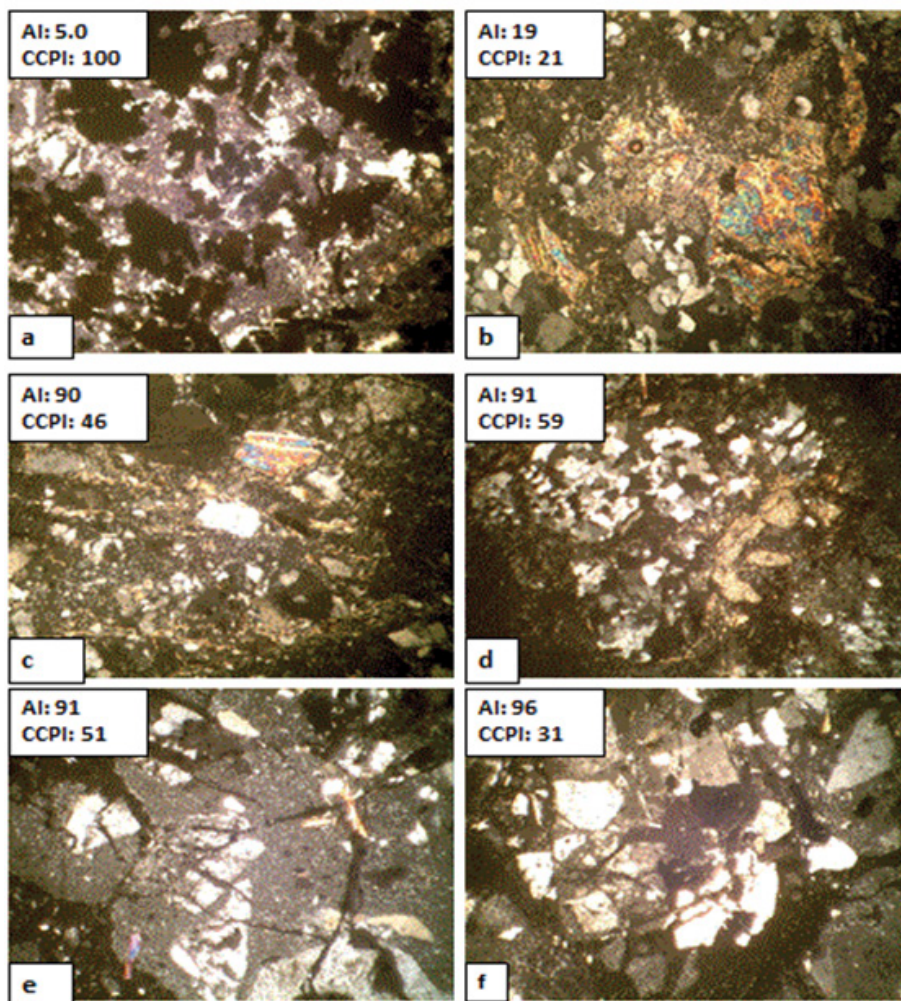


Figure 4: Photomicrograph of granitoids from Kanawa, displaying increasing intensity of hydrothermal alteration (Magnification 40X).

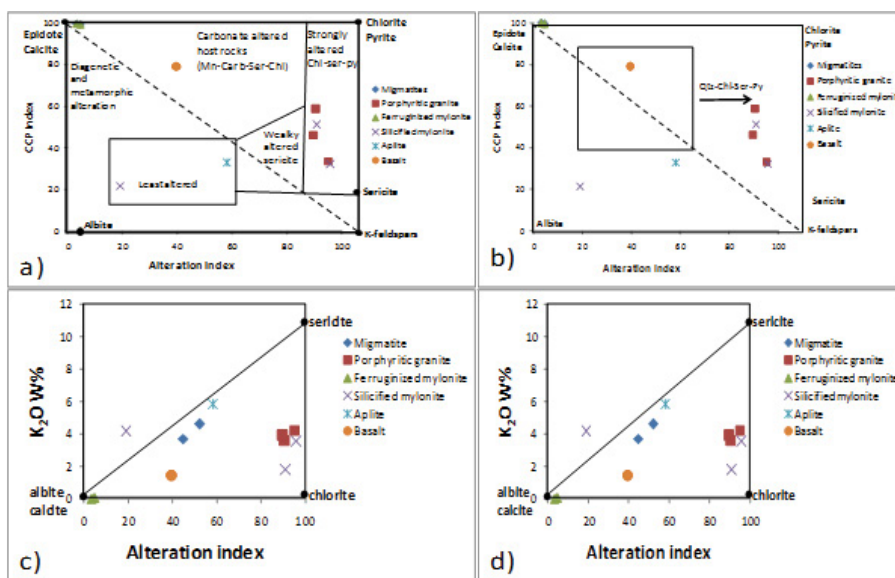


Figure 5: Alteration box plot of Kanawa alteration zones [9]; (a) and (b) showing the degree of alteration; Trends of AI with (c) Na₂O and (d) K₂O.

| Rock | Granite gneiss | | Ferruginised mylonite | | Porphyritic granite | | | Silicified mylonite | | | Aplite | Basalt | | |
|-----------|----------------|------------|-----------------------|------------|---------------------|-------|-------|---------------------|-------|-------|-------------|--------|-------|------|
| Sample | 1 n = 3 | 2 n = 3 | 3 n = 3 | 4 n = 3 | 5 | 6 | 7 | 8 | 9 | 10 | 11 n = 3 | 12 | 13 | 14 |
| La | 80.6 | 149.3 | 62.1 | 61.8 | 74.6 | 92.1 | 59.8 | 27.6 | 33.5 | 36.4 | 87.4 | 27.9 | 29.1 | 28.5 |
| Ce | 178.1 | 296.3 | 150.4 | 151.6 | 141.2 | 170 | 112.4 | 69.9 | 52.6 | 56.7 | 166 | 54.6 | 57.9 | 56.3 |
| Pr | 21.12 | 32.7 | 18.19 | 17.86 | 15.55 | 18.6 | 12.2 | 6.19 | 6.12 | 6 | 21.16 | 6.49 | 6.78 | 6.64 |
| Nd | 83.2 | 113.8 | 86.8 | 82.4 | 53.6 | 65.9 | 42.6 | 23 | 21 | 19.8 | 84.4 | 28.1 | 29.1 | 28.6 |
| Sm | 14.87 | 19.31 | 18.97 | 18.14 | 11.02 | 10.66 | 6.94 | 5.4 | 3.61 | 3.29 | 19.8 | 6.42 | 6.67 | 6.55 |
| Eu | 3.55 | 2.84 | 5.45 | 5.22 | 1.17 | 1.47 | 1.23 | 1.71 | 0.68 | 0.63 | 2.37 | 2.12 | 2.19 | 2.15 |
| Gd | 13.2 | 13.98 | 19.42 | 18.99 | 9.15 | 7.26 | 4.68 | 5.4 | 2.33 | 3.59 | 17.05 | 6.27 | 6.74 | 6.5 |
| Tb | 1.83 | 1.9 | 2.74 | 2.74 | 1.42 | 0.93 | 0.56 | 0.82 | 0.31 | 0.63 | 2.33 | 0.95 | 0.98 | 0.97 |
| Dy | 8.89 | 9.17 | 14.19 | 14.09 | 7.4 | 4.41 | 2.45 | 3.95 | 1.4 | 3.71 | 11.75 | 4.8 | 4.95 | 4.87 |
| Ho | 1.64 | 1.56 | 2.69 | 2.74 | 1.35 | 0.73 | 0.4 | 0.75 | 0.26 | 0.77 | 1.85 | 0.89 | 0.86 | 0.87 |
| Er | 4.37 | 4.15 | 6.6 | 6.86 | 3.56 | 1.92 | 0.76 | 1.71 | 0.72 | 2.14 | 4.5 | 1.93 | 2.22 | 2.08 |
| Tm | 0.59 | 0.56 | 0.91 | 0.87 | 0.48 | 0.29 | 0.11 | 0.23 | 0.1 | 0.3 | 0.61 | 0.26 | 0.27 | 0.26 |
| Yb | 3.65 | 3.49 | 5.46 | 5.57 | 2.67 | 1.92 | 0.75 | 1.49 | 0.66 | 1.84 | 3.3 | 1.48 | 1.5 | 1.49 |
| Lu | 0.55 | 0.46 | 0.82 | 0.79 | 0.39 | 0.29 | 0.1 | 0.21 | 0.09 | 0.28 | 0.43 | 0.22 | 0.21 | 0.22 |
| Total REE | 416.2 | 649.5 | 394.7 | 389.7 | 323.6 | 376.5 | 245 | 148.4 | 123.4 | 136.1 | 423 | 142.4 | 149.5 | 145 |

Table 3: Rare earth element (ppm) data of Wuyo-Gubrunde rocks.

| Criteria | I-type | S-type | Study area |
|-----------------|--|--|---|
| Field | Massive, with little or no foliation contains mafic hornblende-bearing Xenoliths | Usually foliated. Contains meta sedimentary xenoliths. May be associated with regional metamorphism; more likely to be found near their source and shows evidence (migmatite, regional metamorphism) | Augen gneiss, migmatites, highly foliated, highly faulted granites (sheared, altered and zoned) |
| Mineralogical | Hornblende and biotite + accessory magnetite | Biotite, muscovite and cordierite | Biotite, hornblende and very little muscovite |
| Chemical | High Na ₂ O > 3.5% in felsic and > 2.2% in more mafic types. Rich in Ca and poor Rb from the source region. | Low Na ₂ O; normally < 3.5% in rocks with approximately 5% K ₂ O decreasing to > 2.2% in rocks with about 2% K ₂ O. High Al, with high Rb in source rock. | Very low Na ₂ O (0.09-2.73%), K ₂ O (0.03-4.18%) Al ₂ O ₃ (9.81-15.76) and Rb (3.4-243.6 ppm) |
| Ore association | Porphyry copper, Mo | Tin | Uranium |

Table 4: Chappell and white I and S-type granite characteristics compared with the Wuyo-Gubrunde granitoids [10].

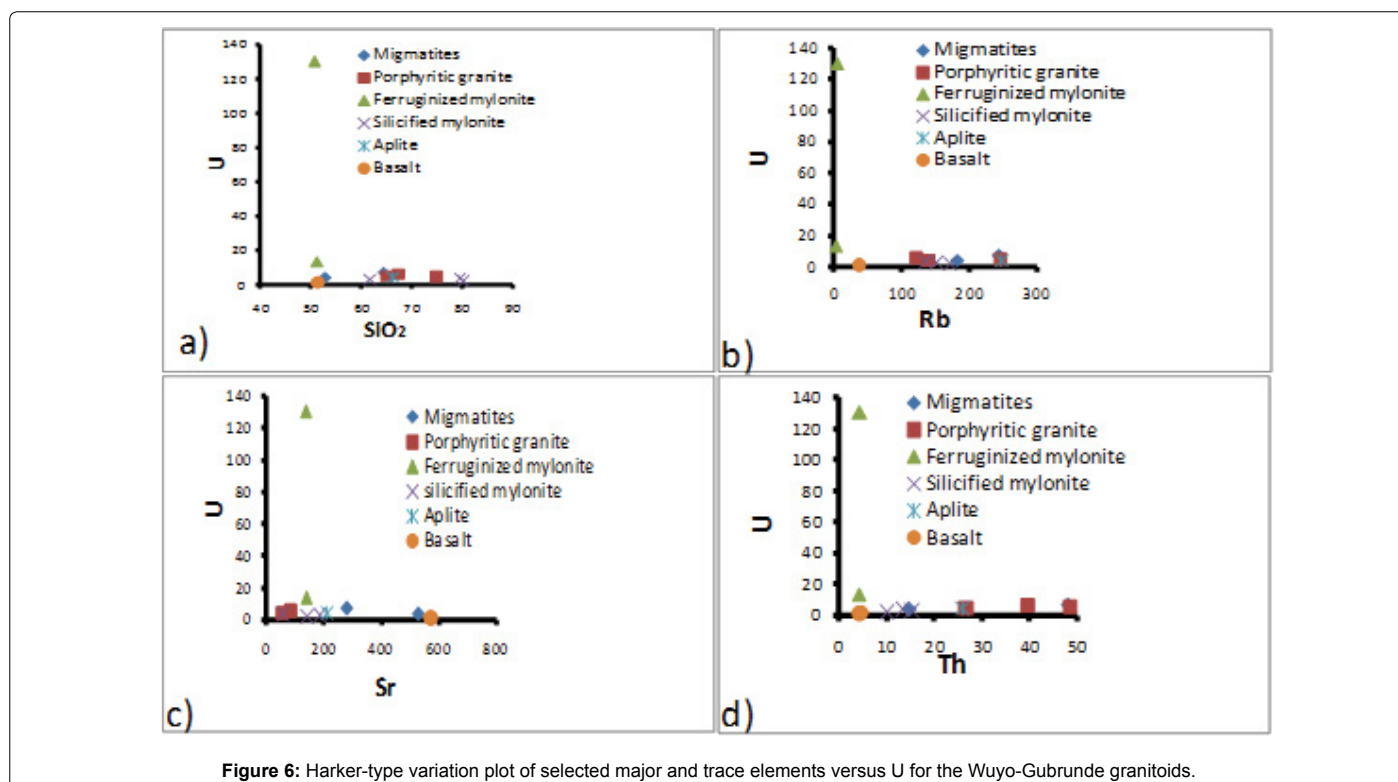


Figure 6: Harker-type variation plot of selected major and trace elements versus U for the Wuyo-Gubrunde granitoids.

| Characteristics | Rössing model | Kanawa model |
|-----------------------------------|--|---|
| Lithology | Pegmatite-alaskite-gneiss; anatectic granite and migmatite | migmatite-gneiss, Porphyritic granite, Medium-grained granite, pegmatites, aplites and basalt |
| Derivation | reworked and recycled sialic crust | reworked crustal material |
| Initial Sr isotopes | >0.710 | NA |
| Levels of emplacement | Catazonal | Catazonal |
| Tectonic stage | Syntectonic | Syntectonic |
| Age | commonly Proterozoic to early Paleozoic | Proterozoic-early Paleozoic (Pan-African age) |
| Tectonic setting | Orogenic | Orogenic |
| Metamorphic rock of country rocks | Middle-upper amphibolites | green-schist and unmetamorphosed |

Table 5: Summary of principal similarities between the Rössing and Kanawa uranium mineralization.

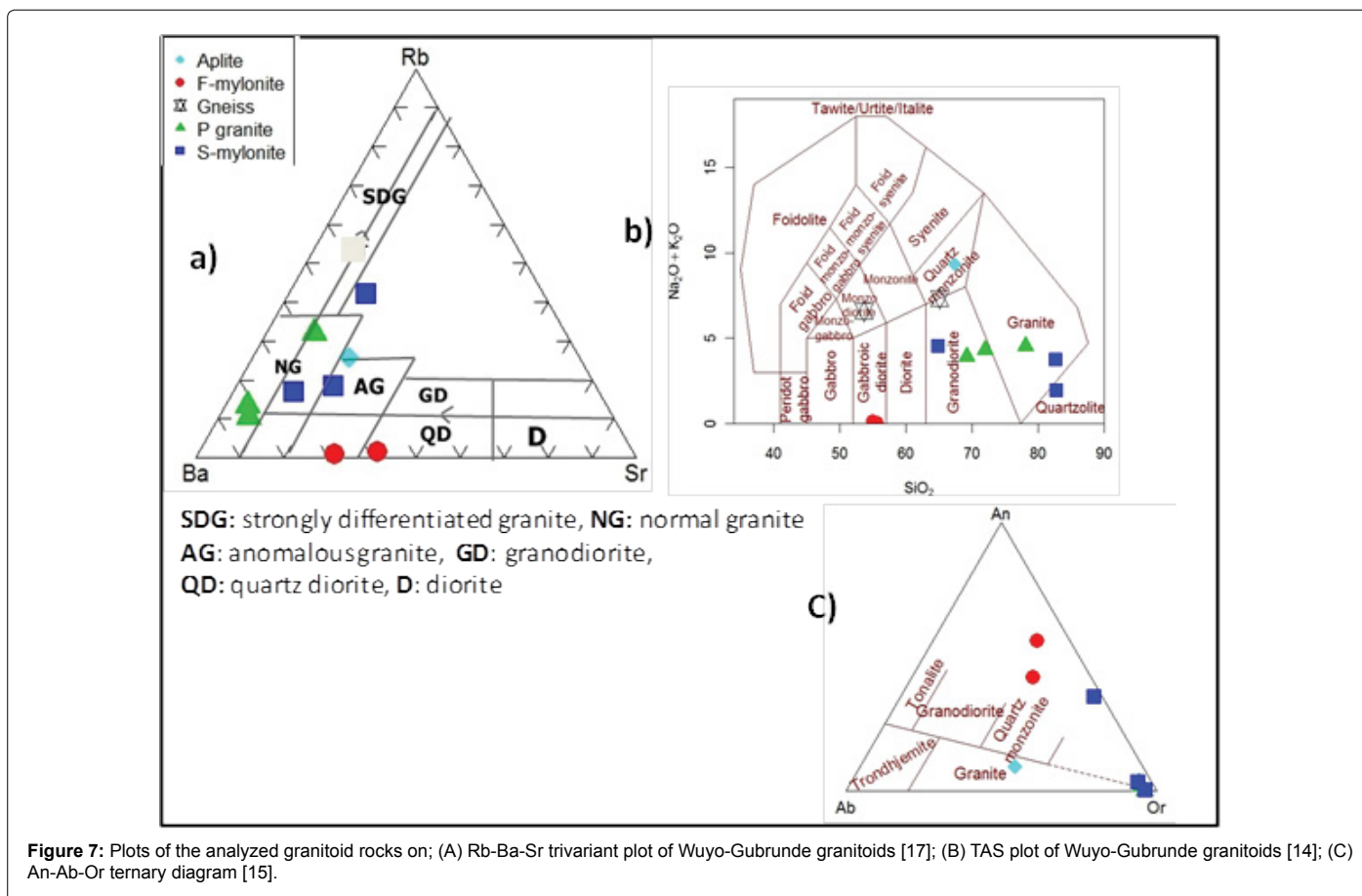


Figure 7: Plots of the analyzed granitoid rocks on: (A) Rb-Ba-Sr trivariant plot of Wuyo-Gubrunde granitoids [17]; (B) TAS plot of Wuyo-Gubrunde granitoids [14]; (C) An-Ab-Or ternary diagram [15].

649 ppm) most of the samples have lower value compared to the total abundances of acid and intermediate rocks (220-350 ppm) [13], suggest original magmatic signatures have been lost due to alteration/remobilizations.

The Rössing deposits of Southwest Africa (Namibia), which is considered to be an ideal example of anatectic remobilization of preexisting sialic crustal material is considered to be an excellent model similar to the Kanawa uranium occurrences (Table 4).

Constraints on the Genesis of the Rock Hosting Wuyo-Gubrunde Uranium

The mineralized portion is situated in the sheared/altered zone trending northerly, dipping almost vertical, bounded side by side by the porphyritic granite. It is fine grained, reddish tectonite. This host rock is been earlier reported as rhyolite [1], which is later argued to be

a deformational product of the granites under oxidizing condition [3]. The plot of Wuyo-Gubrunde granitoids on Rb-Ba-Sr plot, most of the samples cluster in the field of normal-anomalous granites (Figure 7), the ferruginised granite that is mineralized fall in the field of granodiorites and quartz-diorites. Anomalous granite indicates that the rocks have suffered from metasomatism as a result of shearing, anomalous granites may also shift in the field of granodiorite and quartz-diorite as a result of low Rb content, in this case the mineralized altered granite is depleted in Rb (3.4-5.2 ppm) may reflects Rb fractionation during metasomatism. On the TAS plot for volcanic rocks [14], most of the samples cluster in the field of dacite to rhyolites (Figure 7), but the mineralised altered granite falls in the field of basalt due to low silica content (50.83-51.28 wt%), hence it is not rhyolitic. The granitoids can be classified by using normative An-Ab-Or ternary diagram of O'Connor [15]. All the granitoids fall in the field of granites except the ferruginised mylonite which shifts to the field of granodiorites.

Conclusion

A detailed field, petrographic and alteration studies of Kanawa area coupled with geochemistry of the host rock and uranium occurrences. Based on our results we characterize our study area:

1. The Kanawa granitoids are S-type granites, suggesting from partial melting of crustal materials.
2. The sheared zone is highly altered. The alteration products are sericite, chlorite and hematite.
3. The uranium occurrences are epigenetic derived by remobilization from the host rock to the sheared zones, probably through metasomatic process where feldspars have been replaced by U-Fe-Mg in an oxidized condition, the mineralizing fluids may be sourced from the numerous volcanic bodies around the area.
4. The mineralized mylonite is a product of the granitic host. The pathfinder elements of Kanawa uranium occurrences are U-Fe-Mg-Ca-P-Sr-Zr-V-Co.

References

1. Funtua II, Okujeni CD, Abaa SI, Elegba SB (1992) Geology and genesis of uranium mineralization at Kanawa Gubrunde horst, NE. *Nigerian J Mining Geol* 28: 171-177.
2. Funtua II, Okujeni CD, Elegba SB (1999) Preliminary note on the geology and genetic model of uranium mineralization in Northeastern Nigeria. *J Mining Geol* 35: 125-136.
3. Suh CE, Dada SS (1997) Fault rocks and differential reactivity of minerals in the Kanawa violaine uraniumiferous vein, NE Nigeria. *J Struct Geol* 19: 1037-1044.
4. Ojo OM (1982) Geology and stream sediment geochemical survey of middle Gongola Basin (upper Benue trough) of Nigeria. *Nigeria* p: 386.
5. Carter JD, Barber W, Tait EA (1963) The geology of parts of Adamawa, Bauchi and Borno provinces in the Northeastern Nigeria. *Geological Survey of Nigeria Bull* 30: 106.
6. Popoff M (1984) Benue trough oblique rifting and the geodynamic evolution of the Gulf of Guinea. *Revista Brasileira en Geociencias* 18: 315.
7. Zaborski PM, Ugoduluwa F, Idornigie A, Nnbo P, Ibe K (1997) Stratigraphy and structure of the Cretaceous Gongola Basin, North Eastern Nigeria. *Bull Cent Res Explor Product Elf* 21: 153-185.
8. Dike EFC, Egbuniwe IG (1993) An uniformity between the Keri-Keri Formation and basement complex at Mainamiji, Bauchi State. *J Mining Geol* 29.
9. Large RR, Gemell JB, Paulick H (2001) The alteration box plot: A simple approach to understanding the relationship between alteration mineralogy and lithogeochemistry associated with volcanic-hosted massive sulfide deposits. *Eco Geol* 96: 957-971.
10. Chappell BW, White AJR (1978) Granitoids from the Moonbi district, New England batholiths, Eastern Australia. *J Geol Society Australia* 25: 267-283.
11. Bute SI (2015) Geological and geochemical studies of rocks of part of Wuyo-Gubrunde horst, northeastern Nigeria: Implication on uranium occurrences.
12. Steenfelt A (1982) Uranium and selected trace elements in granites from the Caledonides of East Greenland. *Mineral Mag* 46: 201-210.
13. Haskin LA, Schmitt RA (1967) Rare-earth distributions. *Researches in Geochemistry*, John Wiley and Sons, New York.
14. Wilson M (1989) *Igneous petrogenesis*. Unwin Hyman, London.
15. O'Connor JT (1965) A classification for quartz-rich igneous rocks based on feldspars ratios. *US Geol Surv Prof Paper* 525B: B79-B84.
16. Haruna IV, Ahmed HA, Ahmed AS (2012) Geology and tectono-sedimentary disposition of the Bima sandstone of the upper Benue trough (Nigeria): Implications for sandstone-hosted uranium deposits. *J Geol Mining Res* 4: 168-173.
17. El Bouseily AM, El Sokkary AA (1975) The relation between Rb, Ba and Sr in granitic rocks. *Chem Geol* 16: 207-219.